Carcinogenesis vol.31 no.5 pp.794–803, 2010
doi:10.1093/carcin/bgq019
Advance Access publication January 21, 2010

TRPV2 channel negatively controls glioma cell proliferation and resistance to Fas-induced apoptosis in ERK-dependent manner

Massimo Nabissi[1], Maria Beatrice Morelli[1,2], Consuelo Amantini[1], Valerio Farfariello[1,2], Lucia Ricci-Vitiani[3], Sara Caprodossi[1], Antonella Arcella[4], Matteo Santoni[1], Felice Giangaspero[4], Ruggero De Maria[3] and Giorgio Santoni[1,*]

[1]Department of Experimental Medicine and Public Health, University of Camerino, 62032 Camerino (Macerata), Italy, [2]Department of Experimental Medicine, University ''La Sapienza'', 00100 Rome, Italy, [3]Istituto Superiore di Sanità, 00161 Rome, Italy and [4]Istituto di Ricovero e Cura a Carattere Scientifico Istituto Neurologico Mediterraneo Neuromed, 86077 Pozzilli (Isernia), Italy

*To whom correspondence should be addressed. Tel: 39 0737 403312/403319; Fax: 39 0737 403325;
Email: giorgio.santoni@unicam.it

The aim of this study was to investigate the expression and function of the transient receptor potential vanilloid 2 (TRPV2) in human glioma cells. By Real-Time–PCR and western blot analysis, we found that TRPV2 messenger RNA (mRNA) and protein were expressed in benign astrocyte tissues, and its expression progressively declined in high-grade glioma tissues as histological grade increased ($n = 49$ cases), and in U87MG cells and in MZC, FCL and FSL primary glioma cells. To investigate the function of TRPV2 in glioma, small RNA interfering was used to silence TRPV2 expression in U87MG cells. As evaluated by RT-Profiler PCR array, siTRPV2-U87MG transfected cells displayed a marked downregulation of Fas and procaspase-8 mRNA expression, associated with upregulation of cyclin E1, cyclin-dependent kinase 2, E2F1 transcriptor factor 1, V-raf-1 murine leukemia viral oncogene homolog 1 and Bcl-2-associated X protein (Bcl-X_L) mRNA expression. TRPV2 silencing increased U87MG cell proliferation as shown by the increased percentage of cells incorporating 5-bromo-2-deoxyuridine expressing β_{III}-tubulin and rescued glioma cells to Fas-induced apoptosis. These events were dependent on extracellular signal-regulated kinase (ERK) activation: indeed inhibition of ERK activation in siTRPV2-U87MG transfected cells by treatment with PD98059, a specific mitogen-activated protein kinase/extracellular signal-regulated kinase kinase inhibitor, reduced Bcl-X_L protein levels, promoted Fas expression, and restored Akt/protein kinase B pathway activation leading to reduced U87MG cell survival and proliferation, and increased sensitivity to Fas-induced apoptosis. In addition, transfection of TRPV2 in MZC glioma cells, by inducing Fas overexpression, resulted in a reduced viability and an increased spontaneous and Fas-induced apoptosis. Overall, our findings indicate that TRPV2 negatively controls glioma cell survival and proliferation, as well as resistance to Fas-induced apoptotic cell death in an ERK-dependent manner.

Abbreviations: Akt/PKB, Akt/protein kinase B; Bcl-X_L, Bcl-2-associated X protein; BCNU, c1,3-*bis*(2-chloroethyl)-1-nitrosurea; BrdU, 5-bromo-2-deoxyuridine; ERK, extracellular signal-regulated kinase; FACS, fluorescence activated cell sorting; GFAP, glial fibrillary acidic protein; GBM, glioblastoma multiforme; JC-1, 5,5′,6,6,-tetrachloro-1,1′,3,3′-tetraehylbenzimidazolylcarbocyanineiodide; MAPK, mitogen-activated protein kinase; MEK, mitogen-activated protein kinase/extracellular signal-regulated kinase kinase; mTRPV2, mouse ortholog of TRPV2; MTT, 3-(4,5-dimethylthiazol-2-yl)-2,5-diphenyltetrazolium bromide; p38, p38 MAP kinase; Raf-1, V-raf-1 murine leukemia viral oncogene homolog 1; RT, reverse transcription; dxRT–PCR, duplex quantitative real time polymerase chain reaction; TRPV1, transient receptor potential vanilloid type 1; TRPV2, transient receptor potential vanilloid type 2; VP-16, etoposide.

Introduction

Diffusely infiltrating gliomas are the most common primary brain tumors. They are characterized by diffuse infiltration of adjacent brain structure and tendency for progression to anaplasia over the time. Glioblastoma multiforme (GBM) represents the end of the spectrum of malignancy of these neoplasms (1,2). Despite advances in medical and surgical therapies, the outcome for patients diagnosed with GBM remains dismal. Two major features of GBM aggressiveness are high proliferation rate and resistance to chemotherapeutic drug-induced apoptosis (3).

Apoptosis can be triggered by several cell surface receptors belonging to the family of death receptors such as tumor necrosis factor receptor superfamily, member 6 (Fas) and tumor necrosis factor receptors (4). Fas has the ability to interact with the Fas-associated death domain that recruits procaspase-8 to form the death-inducing signalling complex (4,5); in addition, Fas signalling and apoptotic cell death can also be induced in a caspase-8-independent manner (6–8).

The Raf/mitogen-activated protein kinase/extracellular signal-regulated kinase kinase (MEK)/extracellular signal-regulated kinase (ERK) pathway regulates cell proliferation, differentiation, and apoptotic cell death in high-grade gliomas (9). Activation of Ras triggers the downstream serine-threonine kinase V-raf-1 murine leukemia viral oncogene homolog 1 (Raf-1), which in turn activates MEK that phosphorylates and activates p42/p44 mitogen-activated protein kinases (ERK1 and ERK2) (10). ERK1/2 activation then leads to phosphorylation of a variety of substrates and transcription factors that ultimately contribute to induction of gene expression and proliferation (11).

ERK1/2 activation has been also implicated in cellular protection from various apoptotic signals (11,12). Thus, Fas-mediated signalling in Jurkat T cells is abrogated by ERK activation (13), and ERK activity inhibits caspase-8 cleavage but not death-inducing signalling complex assembly (6).

Members of transient receptor potential vanilloid (TRPVs) channel family control cellular homeostasis by regulating calcium influx, cell proliferation, differentiation, and apoptosis; moreover, in the last years, an additional pathophysiological role for TRPV channel family in malignant growth and progression has been demonstrated (14,15). In this regard, we have recently reported a marked loss of transient receptor potential vanilloid type 1 (TRPV1) channel in high-grade gliomas, and TRPV1 involvement in the triggering of p38 MAP kinase (p38) mitogen-activated protein kinase (MAPK)-dependent GBM cell apoptosis in response to its specific agonist, capsaicin (16).

Transient receptor potential vanilloid type 2 (TRPV2), also called vanilloid receptor like-1 (VRL-1), is another member of TRPV cation channel family. Like TRPV1, this receptor is predicted to contain six transmembrane domains, a putative pore-loop region, a cytoplasmic amino terminus with three ankyrin-repeat domains, and a cytoplasmic carboxy terminus (17). TRPV2 shows high Ca^{2+} permeability; functional studies have revealed that TRPV2 responds to noxious heat with an activation threshold of $>52°C$ (17), as well as to changes in osmolarity and membrane stretch (18); in addition, TRPV2 is triggered by agonists such as 2-aminoethoxydiphenyl borate (19), as well as cannabidiol and Δ(9)-tetrahydrocannabinol (20).

Although the gene encoding TRPV2 is highly expressed in the central nervous system (17), TRPV2 transcripts are also found in non-neuronal tissues (17,21–23), suggesting that TRPV2 subserves a relatively broad repertoire of physiological functions.

In non-neuronal cells, TRPV2 channel activity can be regulated by growth factor signalling (24). In this regard, the mouse ortholog of TRPV2 (mTRPV2) is activated by growth factors such as insulin growth factor-I, platelet-derived growth factor, and the neuropeptide

head activator, suggesting a role for TRPV2 in cell growth and the alternative appellation of growth receptor channel. Growth factors induce translocation of TRPV2 channel from the intracellular compartments to the plasma membrane through phosphatidylinositol-3 kinase (PI3 kinase)-dependent and -independent pathways (24,25). In addition, transfection of mTRPV2 in human embryonic kidney 293 cells induces intracellular calcium overload and a PI3-kinase-dependent cell death (25); moreover, myocytes from TRPV2 transgenic mice undergo extensive apoptosis (26). Finally, a role for TRPV2 in migration of prostate cancer cells induced by lysophospholipid stimulation has been reported (27).

Data concerning the function of endogenous TRPV2 have not been provided so far. Herein, we investigated the expression of TRPV2 in glioma cells and tissues, both at messenger RNA (mRNA) and protein levels. Moreover, by employing small RNA interference to knockdown TRPV2 gene expression in U87MG glioma cells, we demonstrated a role for this channel receptor in the control of glioma cell proliferation and resistance to Fas-induced apoptosis, by regulating ERK1/2 activation.

Materials and methods

Cells and tissues

The U87MG glioma cell line (American Type Culture Collection, LGC Promochem, Teddington, UK) and the primary glioblastoma cell lines MZC, FSL, and FCL, derived from bioptic samples surgically removed from patients who gave informed consent to the study, were maintained in modified Eagle's medium supplemented with 10% heat inactivated fetal calf serum, 2mM L-glutamine, 100 IU/ml penicillin, 100 μg streptomycin, non-essential amino acids and 1 mM sodium pyruvate. All cell lines were maintained at 37°C, 5% CO_2 and 95% of humidity. Paraffin-embedded glioma tissues ($n = 49$) and benign astrocyte tissues ($n = 7$) were prepared from bioptic samples surgically removed from patients who gave informed consent to the study. Brain tumors of astrocytic origin were grouped according to malignancy in grade II ($n = 25$), III ($n = 13$), IV ($n = 11$; (World Health Organization classification) (1). Primary glioma cell lines and glioma tissues are available at the human glioma bank INM Neuromed (Pozzilli, Isernia, Italy).

Reagents and antibodies

Etoposide (VP-16), c1,3-*bis*(2-chloroethyl)-1-nitrosurea (BCNU, carmustine), 5-bromo-2-deoxyuridine (BrdU) and the MEK inhibitor PD98059 were purchased from Sigma-Aldrich (St Louis, MO), and Tocris Bioscience (Bristol, UK), respectively. The following mouse monoclonal antibodies (mAbs)were used: anti-β-actin (1:1000; Santa Cruz Biotechnology, Santa Cruz, CA), anti-Fas (1:1000; Sigma-Aldrich), antiphospho ERK (1:1000; Cell Signaling Technology, Danvers, MA), anti-Bcl-X_L (1:200; Santa Cruz Biotechnology), anti-caspase-8 (1:4000; BD Biosciences, San Jose, CA), anti-phospho-p38 MAPK (1:1000; Cell Signaling Technology), anti-β_{III} tubulin (1:100; Cell Signaling Technology), anti-BrdU FITC-conjugated (1:10; BD Biosciences), anti-Fas (clone CH-11) (MBL Corporation, Woburn, MA). The following polyclonal antibodies (Abs) were used: goat anti-TRPV2 (1:200; Santa Cruz Biotechnology), rabbit anti-ERK (1:1000; Santa Cruz Biotechnology), rabbit anti-glial fibrillary acidic protein (GFAP; 1:100; Cell Signaling Technology), rabbit anti-Akt (1:1000; Signalway Antibody, Pearland, TX), rabbit anti-phospho Akt (1:1000; Cell Signaling Technology), rabbit anti-p38 MAPK (1:1000; Cell Signaling Technology), phycoerythrin-conjugated goat antimouse immunoglobulin G (IgG;1:20; BD Biosciences), phycoerythrin-conjugated goat antirabbit-IgG (1:20; BD Biosciences) , horseradish peroxidase-conjugated donkey antigoat IgG (Santa Cruz Biotechnology), horseradish peroxidase-conjugated goat antimouse IgG (1:2000, GE Healthcare Europe GmbH, Milano, Italy), horseradish peroxidase-conjugated donkey antirabbit IgG (1:5000; GE Healthcare) were used as secondary Abs.

Total RNA extraction and complementary DNA synthesis

Total RNA from cell samples and paraffin-embedded sections (5–7 μm thick), was extracted accordingly to the manufacturer's instructions, with the RNeasy Mini Kit (Qiagen GmbH, Hilden, Germany) and the Optimum FFPE RNA isolation kit (Applied Biosystems, Foster City, CA), respectively. Total RNA (100 ng for each sample) was treated with 1 U/ml of DNase I (Qiagen GmbH) and reverse transcribed into complementary DNA (cDNA), in a final volume of 25 μl, using the High-Capacity cDNA Archive Kit (Applied Biosystems). One microliter of the resulting cDNA products was used as template for duplex real-time PCR (dxRT–PCR) quantification.

Probes and primers

DxRT–PCR was performed using human TRPV2 and β-actin probes–primers designed with Primer Premier 5 (Bio-Rad, Hercules, CA) purchased from Sigma-Aldrich. Primers and probes sequences were: β-actin: forward: 5′-GAC ATC CGC AAA GAC CTG TAC G-3′; reverse: 5′-GCC AGG GCA GTG ATC TCC TTC-3′; probe (Fam): 5′-TGC TGT CTG GCG GCA CCA CCA TG-3′; TRPV2: forward: 5′-GCC AAG GAG GGC AAG ATC GAG- 3′; reverse: 5′-CAC AGA AGC CAG GTC ATA CAG C-3′; probe (Texas Red): 5′-ACC CGG ACA GGC CCA TAG CAC CA-3′.

DxRT–PCR analysis

DxRT–PCR was performed using the iQ5 Multicolor Real-Time PCR Detection System (Bio-Rad). The reaction mixture contained the AB RQ Mix for RT–PCR (AB Analitica, Padova, Italy), primer sets (200 nM for β-actin; 400 nM for TRPV2) and probe sets (100 nM for β-actin and 200 nM for TRPV2) in a total volume of 25 μl. Each amplification consisted of heat activation for 3 min at 95°C followed by 40 cycles at 95°C for 1 min and 60°C for 1 min. All samples were assayed in triplicate in the same plate and in three different experiments. Measurement of β-actin levels was used to normalize mRNA contents and TRPV2 levels, calculated by the $2^{-\Delta\Delta Ct}$ method, were expressed as relative fold compared with benign astrocyte tissues used as control.

Cell transfections

siGENOME SMARTpools for TRPV2 (siTRPV2) consisting of four RNA duplex targeting TRPV2 gene, and a siCONTROL non-targeting small interfering RNA (siGLO) with at least four mismatches to any human gene used as negative control, were purchased from Dharmacon (Lafayette, CO). The expression vectors phCMV-FSR was purchased from Genlantis (San Diego, CA). The plasmid encoding human TRPV2 was constructed by introducing in frame TRPV2 cDNA in BglII/HindIII pCMV-FSR cloning sites. For transfection experiments, U87MG and MZC glioma cells were plated at the density of $3 \times 10^4/cm^2$ and after an overnight incubation, 50 nM of siTRPV2 or siGLO and 1 μg/ml of pCMV-TRPV2 or pCMV (empty vector) were added to the wells, following METAFECTENE PRO transfection protocol. Cells were harvested up to day 3 post-transfection for analysis. The efficiency of transfections were evaluated by dxRT–PCR and western Blot analysis.

Cancer pathway finder profile analysis

The Human Cancer Pathway Finder ™ PCR Array and related reagents were purchased from SABiosciences (Frederick, MD). Total RNA from siGLO- and siTRPV2-U87MG transfected cells at day 3 post-transfection was extracted and 2 μg of total RNA from each sample were subjected to reverse transcription in a total volume of 20 μl using the ReactionReady ™ first strand cDNA (SABiosciences). cDNAs were analyzed by quantitative RT–PCR performed using a IQ5 Multicolor Real-time PCR Detection system, the SuperArray's RT^2 real-time SYBR Green PCR Master Mix and the Human Pathways CancerFinder™ (SABioscience) according to manufacturer's instructions. Measurement of two housekeeping genes (β-actin, glyceraldehydes-3-phosphate dehydrogenase) on the samples was used to normalize mRNA content, and the gene expression levels of siTRPV2-transfected cells were expressed as relative fold respect to siGLO-U87MG transfected cells. Data acquisition was performed using the web-based integrated PCR Array Data Analysis Template provided by SABiosciences.

Western blot

Glioma cells and tissues were lysed in lysis buffer (1 M Tris pH 7.4, 1 M NaCl, 10 mM ethyleneglycol-*bis*(aminoethylether)-tetraacetic acid, 100 mM NaF, 100 mM Na_3VO_4, 100 mM phenylmethylsulfonyl fluoride, 2% deoxycholate, 100 mM ethylenediaminetetraacetic acid, 10% Triton X-100, 10% glycerol, 10% sodium dodecyl sulfate, 0.1 M $Na_4P_2O_7$) containing protease inhibitor cocktail (Sigma-Aldrich) by using a Mixer Mill MM300 (Qiagen GmbH). Lysates were separated on sodium dodecyl sulfate polyacrylamide gel (7–12%) and transferred onto Hybond-C extra membranes (GE Healthcare). Non-specific binding sites were blocked with 5% low-fat dry milk in phosphate-buffered saline (PBS) Tween 20 for 1 h at room temperature. Blots were incubated for 1 h with the primary Abs in PBS–Tween 20 supplemented with 3% low-fat dry milk, washed three times with PBS–Tween 20 buffer, and incubated with the appropriate secondary Abs. Immunostaining was revealed by enhanced ECL Western Blotting analysis system (GE Healthcare). Densitometric analysis was performed by ChemiDoc using the Quantity One software (Bio-Rad).

3-(4,5-dimethylthiazol-2-yl)-2,5-diphenyltetrazolium bromide assay

Glioma cells were cultured with different doses of VP-16, BCNU or anti-Fas mAb, alone or in combination, and the percentage of cytotoxicity was measured by 3-(4,5-dimethylthiazol-2-yl)-2,5-diphenyltetrazolium bromide

(MTT) assay. Briefly, 1×10^4 cells per cm^2 were plated in a 96-well plate and then cultured, up to 3 days with the appropriated drugs, in the presence or not of PD98059 (50 μM). Four replicates were used for each treatment. At the indicated time, 0.8 mg/ml of MTT was added to the media and incubated for 3 h. Then the supernatants were discarded and colored formazan crystals, dissolved with 100 μl/well of dimethyl sulfoxide, were read by an enzyme-linked immunosorbent assay reader (BioTek Instruments, Winooski, VT). Sample data are represented as the average of at least three separate experiments.

Immunofluorescence and fluorescence activated cell sorting analysis

BrdU incorporation in U87MG-transfected cells was determined by seeding $3 \times 10^4/cm^2$ cells into six-well plates and assayed at 72 h after transfection. One day before harvesting, cells were labeled by adding 20 μM BrdU. After trypsinization and washing in PBS supplemented with 0.5% bovine serum albumin and 2 mM ethylenediaminetetraacetic acid, cells were fixed for 30 min in PBS solution containing 30% methanol and 0.4 % paraformaldheide, permealized with a PBS solution containing 1% paraformaldheide and 0.01% Tween-20, and then incubated for 15 min in DNAse buffer containing 500 KU/ml of DNAse (Sigma-Aldrich). Thereafter, cells were stained with a 1:10 dilution of anti-BrdU FITC-conjugated Ab, incubated for 1 h at room temperature and washed in PBS solution containing 0.5 % bovine serum albumin and 2 mM ethylenediaminetetraacetic acid. In some experiments, transfected U87MG cells were pulsed for 24 h with BrdU and subsequently stained with FITC-conjugated anti-BrdU mAb, anti-GFAP or anti-β_{III}-tubulin, and their respective phycoerythrin-conjugated goat antirabbit or goat antimouse secondary polyclonal Ab.

Samples were analyzed by a FACScan cytofluorimeter using the CellQuest software (BD Pharmingen, San Diego, CA), and fluorescence intensity was expressed in arbitrary units on logarithmic scale.

Mitochondrial transmembrane potential ($\Delta\Psi_m$), in U87MG-transfected cells, was evaluated by 5,5′,6,6,-tetrachloro-1,1′,3,3′-tetraehylbenzimidazolylcarbocyanineiodide (JC-1) staining. Cells of $1 \times 10^4/cm^2$ were treated with the appropriated drugs, at different concentrations, and then incubated for 10 min at room temperature with 300 μl of 10 μg/ml JC-1. JC-1 was excited by an argon laser (488 nm) and green (530 nm)/red (>570 nm) emission fluorescence was collected simultaneously. Carbonyl cyanide chlorophenylhydrazone protonophore, a mitochondrial uncoupler that collapses ($\Delta\Psi_m$) was used as positive control (data not shown). Samples were analyzed by a FACScan cytofluorimeter using the CellQuest software (BD Pharmingen, San Diego, CA); fluorescence intensity was expressed in arbitrary units on logarithmic scale.

Apoptosis assays

Phosphatidylserine exposure on U87MG and MZC glioma cells was detected by Annexin-V staining and cytofluorimetric analysis. Briefly, $1 \times 10^4/cm^2$ cells were treated with different doses of the appropriated drugs for 72 h in 96-well plates. After treatment, cells were stained with 5 μl of Annexin-V-FITC for 10 min at room temperature and washed once with binding buffer (10 mM HEPES/NaOH, pH 7.4, 140 mM NaCl, 2.5 mM $CaCl_2$).

Statistical analysis

The statistical significance was determined by Student's *t*-test and by Bonferroni post-test (one-way ANOVA; $P < 0.01$).

Results

Expression of TRPV2 mRNA and protein on glioma tissues and cell lines

We determined TRPV2 mRNA expression in glioma tissues with different grades, as well as U87MG and MZC, FCL, and FSL primary glioma cells by dxRT–PCR; we found that TRPV2 mRNA levels were expressed in benign astrocyte control tissues and its expression progressively declined in low- (grade II) versus high-grade gliomas (grades III and IV); furthermore, TRPV2 mRNA expression was markedly reduced in U87MG cells, and strongly downregulated in MZC, FCL, and FSL primary glioma cells as compared with controls (Figure 1A). Consistent with dxRT–PCR data, a progressive reduction of TRPV2 protein expression was evidenced by western blot analysis in glioma tissues as pathological grade increased, with a complete loss in grade IV glioblastomas (Figure 1B), as well as in U87MG and MZC glioma cells (Figure 1C). No reactivity was observed with normal goat serum used as negative control (data not shown).

In conclusion, the loss of TRPV2 expression in high-grade glioblastoma cells and tissues suggests a negative role for TRPV2 in tumor progression.

TRPV2 silencing affects gene expression in U87MG cells

In order to study the functional role of TRPV2 in glioma cells, we silenced TRPV2 gene in U87MG cells by small RNA interference. No changes in cell viability, morphology, and adhesive properties were observed in transfected versus untransfected U87MG cells (data not shown). As evaluated by dxRT–PCR, a progressive decrease of TRPV2 mRNA levels from day 1 up to day 4 post-transfection was observed in siTRPV2-transfected cells, with a marked loss detected already at day 2 (Figure 2A); similarly, western blot analysis revealed a parallel decrease of TRPV2 protein at day 3 (Figure 2B). No major differences in TRPV2 mRNA expression were observed in siGLO-transfected cells.

Thereafter, we investigate the role of TRPV2 in glioma cells, by evaluating the expression of 84 genes representative of six biological pathways involved in transformation and tumorigenesis, in siTRPV2- and siGLO-U87MG transfected cells by performing an RT-Profiler

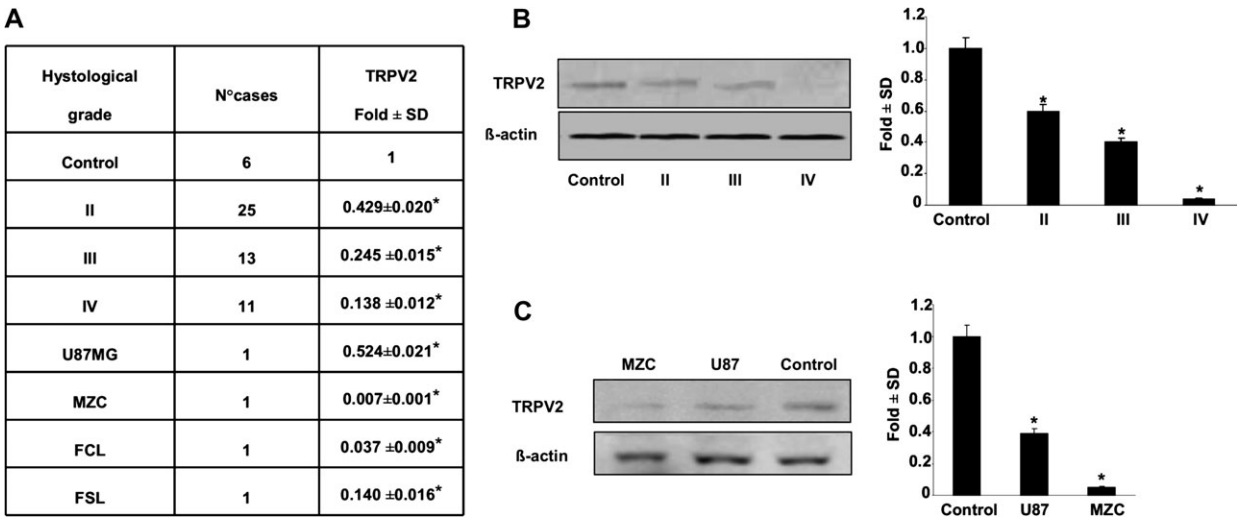

Fig. 1. TRPV2 expression in human glioma cells and tissues. (**A**) Analysis of TRPV2 gene expression in glioma cells and tissues grouped according the grade of malignancy was performed by dxRT–PCR. RNA from benign tumor tissues were used as control. Values, normalized for β-actin expression, were expressed as fold change with respect to control. Statistical analysis was performed comparing tissues and cell lines with control, $^*P < 0.01$. (**B, C**) A representative western blot analysis of TRPV2 protein levels in glioma tissues and cells. Benign tumour tissues were used as control. β-actin protein levels were evaluated as loading control. Data are expressed as fold change with respect to control. Statistical analysis was performed comparing MZC and U87 cell lines with control,$^*P < 0.01$.

A

siTRPV2 transfection days	TRPV2 relative expression (Fold ± SD)
0	1
1	0.41 ± 0.02*
2	0.08 ± 0.01*
3	0.08 ± 0.01*
4	0.13 ± 0.01*

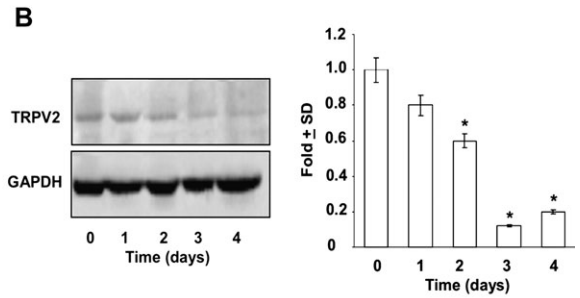

C

Gene Bank	Symbol	Description	Fold ± SD
NM 138578	BCL2L1	BCL2-like 1 (Bcl-X_L)	16.3 ± 0.11
NM 000043	FAS	Fas (TNF receptor superfamily, member 6)	-11.4 ± 0.20
NM 001228	CASP 8	Caspase 8, apoptosis-related cysteine protease	-2.7 ± 0.02
NM001238	CCNE 1	Cyclin E1	2.5 ± 0.08
NM001798	CDK2	Cyclin-dependent kinase 2	2.1 ± 0.09
NM 005225	E2F1	E2F transcription factor 1	11.1 ± 0.22
NM 002880	RAF 1	V-raf-1 murine leukemia viral oncogene homolog 1	2.6 ± 0.02

Fig. 2. Cancer pathways related genes affected by TRPV2 gene silencing in U87MG cells. (**A**) TRPV2 mRNA levels were evaluated by dxRT–PCR in siTRPV2-U87MG transfected cells at different transfection times (0–4 days). Relative TRPV2 expression, normalized to β-actin mRNA levels, were calculated using day 0 of transfection as calibrator. Statistical analysis was performed comparing transfection times with day 0, $^*P < 0.01$. (**B**) Lysates from siTRPV2-U87MG transfected cells were separated on sodium dodecyl sulfate–polyacrylamide gel electrophoresis and probed with specific goat antihuman TRPV2 Ab. Glyceraldehydes-3-phosphate dehydrogenase protein levels were evaluated as loading control. Relative TRPV2 expression values were calculated using day 0 as calibrator. Data shown are the mean ± SD of three separate experiments. Statistical analysis was performed comparing transfection times with day 0, $^*P < 0.01$. (**C**) The RT profiler PCR array in mRNA samples extracted from siTRPV2 and siGLO-U87MG at day 3 post-transfection. Right column represent fold differences of individual gene expression between siTRPV2- and siGLO (calibrator)-U87MG cells. The expression levels were normalized to the average Ct value of two housekeeping genes (β-actin and glyceraldehydes-3-phosphate dehydrogenase), calculated by the ΔΔCt method and expressed as fold change from calibrator. Table includes genes whose expression is, at least, two-fold up- or downregulated in siTRPV2-U87MG transfected cells.

PCR array using a customized Cancer Pathway Finder PCR array. TRPV2 silencing significantly modulated the expression of genes controlling cell cycle, proliferation and apoptosis being five genes upregulated and two genes downregulated. Among them, expression of cyclin E1, cyclin-dependent kinase 2, E2F1 transcriptor factor 1, Raf-1 and the anti-apoptotic Bcl-X_L genes was increased, whereas reduced expression of death receptor apoptosis-related genes, such as Fas and procaspase-8, was observed (Figure 2C).

Overall, our data indicate that silencing of TRPV2 in U87MG cells promotes a genetic program favoring cell proliferation and survival, thus suggesting that this receptor negatively controls glioma growth and progression.

ERK phosphorylation is increased in TRPV2-silenced U87MG cells

Our finding that Raf-1 mRNA is upregulated in siTRPV2-U87MG cells together with the major role described for ERK1/2 and p38MAP kinases in the control of glioma cell proliferation and apoptosis (9,16) prompted us to evaluate the ERK1/2 phosphorylation status in siTRPV2-U87MG transfected cells. We found enhanced ERK phosphorylation in siTRPV2-U87MG transfected cells, which was completely inhibited by the specific pharmacological MEK inhibitor PD98059 (Figure 3A). As previously described, ERK was phosphorylated at basal level in U87MG cells (28); no statistically significant changes in ERK protein and phosphorylation levels were found in PD98059-treated compared with siGLO-U87MG cells (Figure 3A). In regard to p38MAPK, it was phosphorylated at basal level; however, no changes in phosphorylation status was found in siTRPV2-U87MG transfected cells as compared with siGLO control cells (Figure 3B)

Overall, these results demonstrate that TRPV2 silencing results in ERK activation and suggest its involvement in the control of glioma cell proliferation and survival.

Decreased Fas expression, Akt/protein kinase B phosphorylation, and increased Bcl-X_L expression in TRPV2-silenced U87MG cells are ERK dependent

ERK activation has been shown to prevent Fas-mediated apoptosis (6,13) and to regulate cell death at mitochondrial level by modulating Bcl-X_L expression (24,29). In addition, increased ERK phosphorylation and reduced sensitivity of cancer cells to chemotherapeutic drug-mediated apoptosis is induced by inhibition of PI3K/Akt pathway (30) that is mainly involved in the control of cell survival (31).

Thus, we evaluated whether the changes in Fas, procaspase 8 and Bcl-X_L expression observed in siTRPV2-U87MG transfected cells were dependent on ERK activation. In accordance with mRNA expression (Figure 2C), marked increase of Bcl-X_L protein expression, associated with a decrease in Fas and procaspase-8 protein levels, was detected by immunoblot in cell lysates from siTRPV2-U87MG transfected cells (Figure 3C), whereas no changes were found in siGLO-U87MG transfected cells (data not shown). Moreover, PD98059, at the dose that completely inhibited ERK phosphorylation, reverted the induced downregulation of Fas and markedly reduced Bcl-X_L overexpression in siTRPV2 glioma cells (Figure 3C). Neither changes of

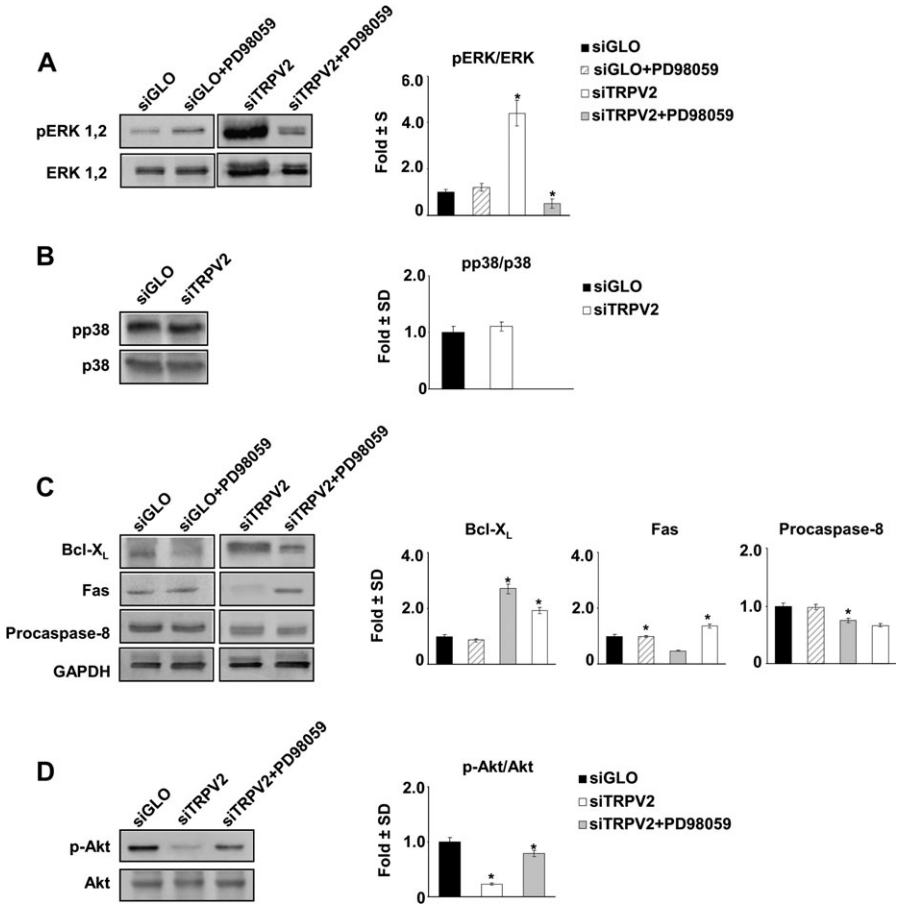

Fig. 3. TRPV2 gene silencing affects ERK phosphorylation and PD98059 inhibits siTRPV2-induced modulation of Fas, Bcl-X_L and Akt phosphorylation level in U87MG cells. (**A**) siTRPV2 transfection induces increase of ERK phosphorylation. Lysates from siGLO- and siTRPV2-U87MG transfected cells were separated on sodium dodecyl sulfate–polyacrylamide gel electrophoresis and probed with specific antihuman pERK and ERK Abs. pERK expression levels were normalized with respect to ERK protein levels. (**B**) Lysates from siGLO- and siTRPV2-U87MG transfected cells, at day 3 post-transfection, were separated on sodium dodecyl sulfate–polyacrylamide gel electrophoresis and probed with specific antihuman anti-phospho-p38 MAPK (pp38) and p38 Abs. pp38 expression levels were normalized with respect to p38 protein levels. (**C**) Lysates from siGLO- and siTRPV2-U87MG transfected (untreated or treated with PD98059) cells, at day 3 post-transfection, were separated on sodium dodecyl sulfate–polyacrylamide gel electrophoresis and probed with specific antihuman Bcl-X_L, Fas, procaspase-8 Abs. Glyceraldehydes-3-phosphate dehydrogenase protein levels were evaluated as loading control. (**D**) Lysates were also probed with specific antihuman pAkt and Akt Abs. Akt protein levels were evaluated as loading control. Data shown are the means ± SD of three biological repeats and are expressed as fold change with respect to siGLO. Statistical analysis was performed comparing siTRPV2 with siGLO and siTRPV2 plus PD98059 with siTRPV2-U87MG transfected cells ($^*P < 0.01$).

procaspase-8 protein expression nor caspase-8 activation were found in PD98059-treated siTRPV2-U87MG transfected cells (Figure 3C). No significant difference in Bcl-X_L, Fas, and procaspase-8 protein expression were found in PD98059-treated versus untreated siGLO-U87MG transfected cells used as control (data not shown).

We also evaluated the role of ERK activation in the control of PI3-kinase pathway in siTRPV2-U87MG transfected cells by evaluating the phosphorylation of the downstream effector molecule Akt/PKB. A basal level of Akt/PKB phosphorylation was observed siGLO-U87MG transfected cells that was strongly reduced upon TRPV2 silencing. This inhibition was completely reverted by PD98059 treatment (Figure 3D).

Overall, our findings indicate that ERK activation following TRPV2 silencing, alters the balance between proapoptotic and anti-apoptotic signals in that it decreases Fas expression and PI3K/Akt activation and parallelly increases Bcl-X_L expression.

TRPV2 silencing increases survival and proliferation of U87MG glioma cells

As decreased expression of TRPV2 by small RNA interfering resulted in transcriptional activation of genes controlling cell survival and proliferation, as well as increased ERK phosphorylation, we evaluated the viability and proliferation of siTRPV2- and siTRPV2- and siGLO-U87MG transfected cells by MTT and BrdU incorporation assays, respectively.

Augmented glioma cell viability was evidenced in siTRPV2 cells as compared with siGLO cells (Figure 4A) and was associated with an increased percentage of cells incorporating BrdU (Figure 4B). We further characterized the phenotype of proliferating U87MG cells by analyzing the expression of astrocytic GFAP and neuronal β_{III}-tubulin markers on BrdU-positive cells. FACS analysis revealed a significant increase in the percentage of proliferating BrdU$^+\beta_{III}$-tubulin$^+$ but not in BrdU$^+$GFAP$^+$ siTRPV2 U87MG cells with respect to siGLO control cells (Figure 4C and D).

We also evaluated the role of ERK activation in the control of enhanced siTRPV2-U87MG transfected cells proliferation, using the MEK inhibitor PD98059. A decrease cell viability and percentage of BrdU$^+$ cells was evidenced only in PD98059-treated siTRPV2-U87MG transfected cells compared with untreated cells (Figure 4A and B), being both U87MG GFAP$^+$ and β_{III}-tubulin$^+$ proliferating cell populations inhibited (Figure 4C and D). Overall, these results suggest ERK activation is a major event controlling the enhanced U87MG cell proliferation upon TRPV2 silencing.

TRPV2 silencing protects U87MG cells from ERK-dependent apoptosis induced by Fas in combination with chemotherapeutic treatment

U87MG glioma cells express the death receptor Fas and are moderately sensitive to apoptosis induced by its triggering (32). Thus, we evaluated the effects of specific mAb-mediated Fas triggering in

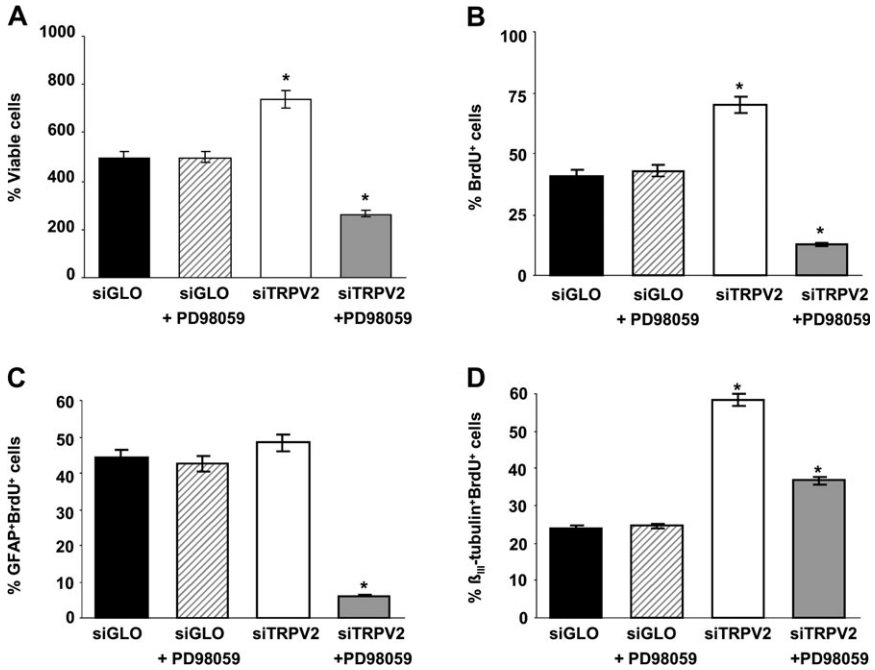

Fig. 4. PD98059 inhibits the siTRPV2-induced increase of proliferation in U87MG cells. *(***A**) The percentage of viable cells from siGLO- and siTRPV2-U87MG transfected cells (untreated or treated with 50 μM of PD98059) cells was determined by MTT assay. (**B**) The percentage of $BrdU^+$ cells from siGLO- and siTRPV2-U87MG transfected cells (untreated or treated with 50 μM of PD98059) cells was determined by pulsing cells 24 h before analysis with 20 μM BrdU and then was analyzed its incorporation at day 3 post- transfection. (**C, D**) The percentage of $BrdU^+$ $GFAP^+$ or $BrdU^+$ β_{III}-$tubulin^+$ cells was evaluated by staining BrdU-pulsed siGLO- and siTRPV2-U87MG transfected (untreated or treated with 50 μM of PD98059) cells with anti-GFAP or anti-β_{III}-tubulin Abs followed by their respective phycoerythrin-conjugated secondary Abs and FITC-conjugated anti-BrdU Ab. Data shown are the mean ± SD of three separate experiments. Statistical analysis was performed comparing siTRPV2 with siGLO and siTRPV2 or siGLO plus PD98059, respectively, with siTRPV2 or siGLO-U87MG transfected cells ($^*P < 0.01$).

siTRPV2-U87MG transfected cells. Treatment of siGLO glioma cells with anti-Fas mAb triggered apoptosis, as measured by MTT and Annexin-V assay, whereas siTRPV2-U87MG transfected are completely resistant to anti-Fas mAb-mediated effects (Figure 5A). Then, we evaluated the effects of the combined treatment with anti-Fas mAb (250 ng/ml) and a suboptimal dose of VP-16 (50 μM) or BCNU (100 μM), on apoptotic cell death. We found that Fas triggering in combination with drug treatment did not augment the sensitivity of siTRPV2-U87MG transfected cells to apoptotic cell death, whereas it exerted proapoptotic effects in siGLO-U87MG transfected cells (Figure 5B and C). In addition, according to previously report (33), we suggested that overexpression of Bcl-X_L in siTRPV2-U87MG transfected cells conferred less sensitivity of siTRPV2-U87MG transfected cells to both VP-16 and BCNU as compared with siGLO control cells (Supplementary Figure 1 is available at *Carcinogenesis* Online).

We also evaluated whether inhibition of enhanced ERK activation in siTRPV2-U87MG transfected cells by PD98059 treatment promoted apoptosis and sensitized these cells to Fas-induced cell death. Treatment of siTRPV2-U87MG transfected cells with PD98059 reduced cell viability (4.1 ± 0.3% versus 28.3 ± 2.0%) and induced mitochondrial-dependent apoptosis as shown by the increase in the percentage of Annexin-V^+cells (3.4 ± 0.3% versus 26.3 ± 2.5%) and of cells showing $\Delta\Psi_m$ dissipation (8.6 ± 0.4 versus 28.1 ± 0.8%). Moreover, siTRPV2-U87MG transfected cells became more sensitive to apoptosis induced by anti-Fas mAb used alone or in combination with VP-16 or BCNU, following inhibition of ERK activation (Figure 5D, E and F).

Overall, our results indicate that inhibition of ERK activation sensitizes siTRPV2-U87MG transfected cells to mitochondrial-dependent apoptosis induced by Fas in combination with chemotherapeutic treatment.

TRPV2 transfection reduces survival, increases spontaneous apoptosis and sensitises MZC glioma cells to Fas- and chemotherapy-induced effects

To further provide evidences on the role of TRPV2 in survival, proliferation, and sensitivity of glioma cells to Fas and chemotherapy-mediated effects, we transiently transfected MZC glioma cells with TRPV2 cDNA cloned in pCMV vector (pCMV-TRPV2) (Figure 6A and B) and evaluated the effects of TRPV2 transfection by MTT and Annexin-V assays. We found that enforced TRPV2 expression in MZC glioma-tranfected cells resulted in a reduced survival and an increased spontaneous and chemotherapy-induced apoptosis as compared with pCMV-MZC-transfected control cells (Figure 6 C, D and E). Moreover, TRPV2 transfection in MZC glioma cells, by inducing Fas overexpression, confers increased sensitivity to Fas-induced apoptosis (Figure 6F).

Overall, these results strengthened the negative role played by TRPV2 in the control of glioma cell survival and proliferation as well as resistance to Fas-induced apoptotic cell death.

Discussion

Malignant cell transformation resulting from enhanced proliferation, aberrant differentiation, and resistance to apoptotic cell death is responsible for abnormal tissue growth, which can eventually turn into uncontrolled expansion and invasion, characteristics of cancer. Such transformation is often accompanied by changes in ion channel expression, and consequently by alterations of the cellular responses that they mediate (15).

Human glioma cells express a variety of ion channels (34,35), including TRPV1 channel (16). Herein, we provide evidence on the expression of TRPV2 by glioma cells and tissues and its involvement in ERK-dependent regulation of glioma cell proliferation and susceptibility to Fas-induced apoptosis.

As evaluated by RT–PCR, TRPV2 mRNA and protein were expressed in benign astrocyte tissues; in addition, TRPV2 expression progressively decreased in U87MG and MZC glioma cells and tissues as pathological grade increased, with a marked reduction of TRPV2 in high-grade gliomas.

In conclusion, the loss of TRPV2 mRNA and protein expression in high-grade glioblastomas suggests a negative role for TRPV2 in tumor progression.

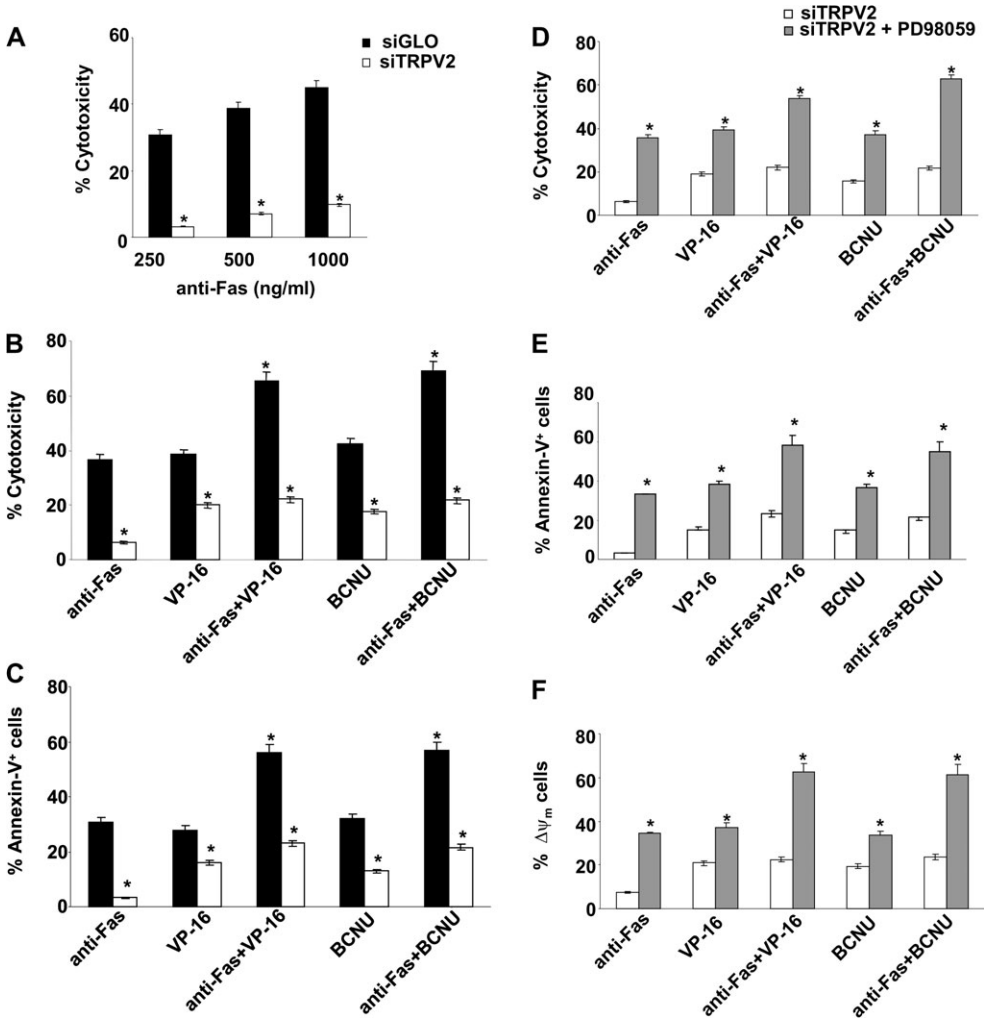

Fig. 5 PD98059 stimulates anti-Fas and/or VP-16 and BCNU-induced mitochondrial-dependent apoptosis of siTRPV2-U87MG transfected glioma cells. (**A**) TRPV2 gene silencing inhibits anti-Fas mAb-induced apoptosis in U87MG glioma cells. siGLO and siTRPV2-transfected cells were treated with different concentration of anti-Fas mAb for 3 days. The percentage of cytotoxicity was determined by MTT assay. Data shown are the mean ± SD of three separate experiments. Statistical analysis was performed comparing siTRPV2 with siGLO, $^{*}P < 0.01$. (**B**) The percentage of cytotoxicity of siGLO- and siTRPV2-U87MG transfected cells treated, for 3 days, with anti-Fas mAb (250 ng/ml), VP-16 (50 μM), BCNU (100 μM) alone or in combination was determined by MTT assay. Data shown are the mean ± SD of three separate experiments. Statistical analysis was performed comparing anti-Fas mAb or VP-16 or BCNU-treated with anti-Fas mAb plus VP-16 or BCNU-treated siGLO-U87MG transfected cells ($^{*}P < 0.01$) and siTRPV2 with siGLO ($^{*}P < 0.01$). (**C**) The percentage of Annexin-V^{+} in siGLO and siTRPV2-U87MG transfected cells, treated as above described, was evaluated by immunofluorescence and fluorescence activated cell sorting (FACS) analysis. Data shown are the mean ± SD of three separate experiments. Statistical analysis was determined comparing anti-Fas mAb or VP-16 or BCNU-treated with anti-Fas mAb plus VP-16 or BCNU-treated siGLO-U87MG transfected cells ($^{*}P < 0.01$) and siTRPV2- with siGLO-U87MG transfected cells ($^{*}P < 0.01$). (**D**) The percentage of cytotoxicity in siTRPV2-U87MG transfected glioma cells, treated for 3 days with anti-Fas mAb (250 ng/ml), VP-16 (50 μM), BCNU (100 μM), alone or in combination, and in the presence or not of PD98059 (50 μM), was determined by MTT assay. Data shown are the mean ± SD of three separate experiments. Statistical analysis was performed comparing PD98059-treated siTRPV2- with siTRPV2-U87MG transfected cells ($^{*}P < 0.01$). (**E**) The percentage of Annexin-V^{+} in siTRPV2-U87MG transfected glioma cells, treated for 3 days as above described, was determined by immunofluorescence and FACS analysis. Data shown are the mean ± SD of three separate experiments. Statistical analysis was performed comparing PD98059-treated siTRPV2- with siTRPV2-U87MG transfected U87 cells ($^{*}P < 0.01$). (**F**) Changes of $\Delta\Psi_m$ were evaluated in siTRPV2-U87MG transfected cells, treated as above described, by JC-1 staining and biparametric FL1 (green)/FL2 (red) flow cytometric analysis. Numbers indicate the percentage of gated siTRPV2-U87MG transfected cells showing a drop in $\Delta\Psi_m$-related red fluorescence intensity. Data shown are the mean ± SD of three separate experiments. Statistical analysis was performed comparing PD98059-treated siTRPV2- with siTRPV2-U87MG transfected cells ($^{*}P < 0.01$).

In order to explore the molecular mechanisms underlying the functional role of endogenously expressed TRPV2 in the control of glioma cell proliferation and survival, we silenced TRPV2 gene in U87MG cells by RNA interference.

By using a customized PCR array, we found that silencing of TRPV2 gene altered the expression of seven genes regulating glioma cell proliferation and apoptotic cell death. TRPV2 silencing resulted in upregulation of the cyclin E1, cyclin-dependent kinase 2, and E2F1 transcriptor factor 1 genes controlling G1 to S phase transition, the antiapoptotic Bcl-2 member, Bcl-X_L, and of Raf-1 kinase that transduces mitogenic and prosurvival signals (9). In addition, marked downregulation of the proapoptotic death receptor Fas and procaspase-8 genes was also detected in TRPV2 siRNA-transfected U87MG cells.

Modulation of genes promoting cell proliferation and survival by TRPV2 silencing was accompanied by a marked increase in U87MG cell survival and proliferation, as assessed by MTT and BrdU incorporation assays. The increased proliferation was mainly sustained by cells expressing the neuronal β_{III}-tubulin marker with respect to GFAP^{+} cells of astrocytic origin. Notably, β_{III}-tubulin is not only an early neuronal marker but it is also highly expressed in diffuse astrocytic glioma and glioblastomas with an ascending grade of

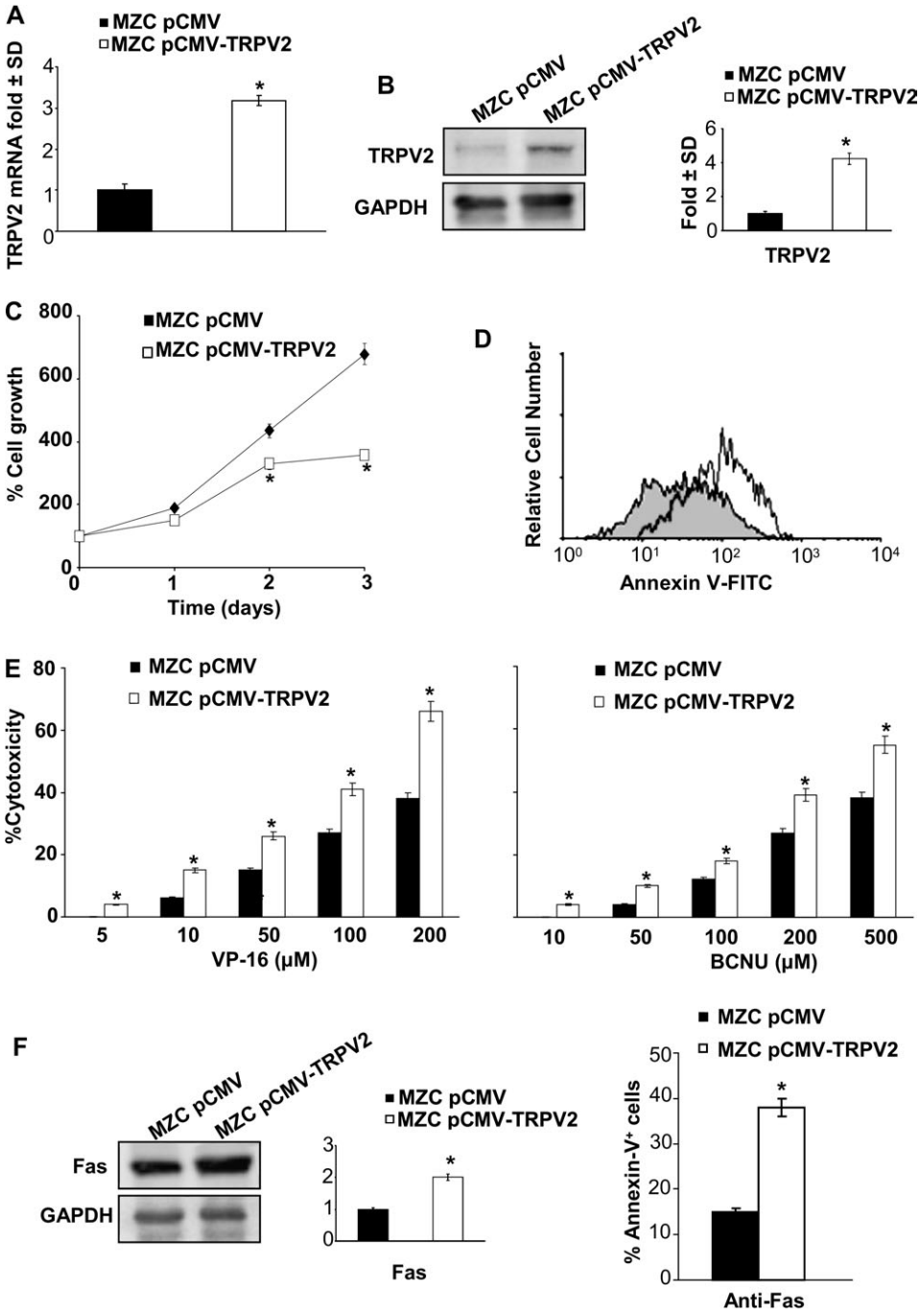

Fig. 6. TRPV2 transient transfection in MZC primary glioma cell line. (**A**) TRPV2 mRNA levels were evaluated by dxRT–PCR in MZC pCMV (empty vector) and MZC pCMV-TRPV2 (TRPV2 encoding vector) transfected cells, 3 days post-transfection. Relative TRPV2 expression, in MZC pCMV-TRPV2 cells, normalized to β-actin mRNA levels, were calculated using MZC pCMV as calibrator. Data shown are the mean ± SD of three separate experiments. Statistical analysis was performed comparing MZC pCMV-TRPV2 with MZC pCMV cells, $^{*}P < 0.01$. (**B**) Lysates from MZC-transfected cells were separated on sodium dodecyl sulfate–polyacrylamide gel electrophoresis and probed with specific goat antihuman TRPV2 Ab. glyceraldehydes-3-phosphate dehydrogenase protein levels were evaluated as loading control. Relative TRPV2 expression values were calculated using MZC pCMV as control. Statistical analysis was performed comparing MZC pCMV-TRPV2 with MZC pCMV cells, $^{*}P < 0.01$. (**C**) Cell growth of MZC-transfected cells was determined by MTT assay. Data shown are the mean ± SD of three separate experiments. Statistical analysis was performed comparing MZC pCMV-TRPV2 with MZC pCMV cells, $^{*}P < 0.01$. (**D**) The percentage of Annexin-V^{+} in MZC pCMV (gray area) and MZC pCMV-TRPV2 (white area) was evaluated by immunofluorescence and fluorescence activated cell sorting (FACS) analysis. (**E**) VP-16 and BCNU dose response in MZC-transfected cells. Cell viability was determined by MTT assay. Data shown are the mean ± SD of three separate experiments. Statistical analysis was performed comparing MZC pCMV-TRPV2 with MZC pCMV cells, $^{*}P < 0.01$. (**F**) (Left panel) Lysates from MZC pCMV and MZC pCMV-TRPV2 transfected cells were separated on sodium dodecyl sulfate–polyacrylamide gel electrophoresis and probed with antihuman Fas mAb. Glyceraldehyde-3-phosphate dehydrogenase protein levels were evaluated as loading control, (right panel). The percentage of Annexin-V^{+} in MZC pCMV and MZC pCMV-TRPV2 transfected cells, treated with anti-Fas mAb (250 ng/ml), was evaluated by immunofluorescence and FACS analysis. Data shown are the mean ± SD of three separate experiments. Statistical analysis was performed comparing MZC pCMV-TRPV2 with MZC pCMV cells, $^{*}P < 0.01$.

histological malignancy and with correspondingly high proliferative indices (36). In addition, as evaluated by MTT and Annexin-V assays, enforced expression of TRPV2 on low TRPV2-expressing MZC glioma cells resulted in a marked inhibition of cell survival and enhancing of spontaneous apoptosis. Accordingly, myocytes from mTRPV2 transgenic mice undergo spontaneously to massive apoptosis (26).

Glioma cells are moderately sensitive to Fas-induced cell death (32); this sensitivity might be increased by treatment with some antitumor chemotherapeutic agents (37). Our results provide evidence that, in accordance with down-modulation of Fas expression and upregulation of Bcl-X_L, TRPV2 silencing in U87MG cells increased their resistance to apoptotic cell death triggered by anti-Fas-specific mAb used alone or in combination with suboptimal doses of anticancer agents such as VP-16 and BCNU, as shown by the decreased percentage of Annexin-V-positive cells (37).

These findings are in agreement with the increased sensitivity to Fas-induced apoptosis that we evidenced in TRPV2-transfected MZC glioma cells.

ERK activation is a key event controlling survival and proliferation of different cancer cells including glioma (38). ERK activation has been shown to prevent Fas-mediated apoptosis in Jurkat T cells (6–8,13,39); conversely, inhibition of ERK activation increases Fas expression, promotes the apoptosis of Raf-1 overexpressing lymphomas and solid tumor cells (40), and sensitizes HeLa cells to Fas receptor-mediated apoptosis (6). In addition, increased ERK phosphorylation and reduced sensitivity of cancer cells to chemotherapeutic drug-mediated apoptosis is induced by inhibition of PI3K/Akt pathway (31) that is mainly involved in the control of cell survival (32).

We have demonstrated that TRPV2 silencing of U87MG cells is associated with Raf-1 mRNA upregulation and increased ERK phosphorylation; this increase was abrogated by using the specific pharmacological MEK inhibitor PD98059, thus suggesting that impaired TRPV2 expression results in ERK activation. We therefore evaluated the involvement of ERK activation in the survival and proliferation of siTRPV2-U87MG transfected cells and we found that inhibition of ERK activation by PD98059 treatment markedly reduced cell viability and the percentage of BrdU-positive proliferating cells in siTRPV2-U87MG transfected cells. Our findings are consistent with previous results showing that the ERK1/2 activation inhibitor U0126 reduces the proliferation of rat C6 glioma cells (41). Moreover, PD98059 significantly increased Fas expression and triggering in siTRPV2-U87MG transfected cells. Accordingly, inhibition of ERK activation was associated with an increased sensitivity of siTRPV2 glioma cells to Fas-induced apoptosis, with the maximal effects observed by using anti-Fas mAb in combination with VP-16 or BCNU. The increased sensitivity of Fas-triggered siTRPV2-U87MG transfected cells to the proapoptotic effects exerted by the chemotherapeutic agents may be attributable to the ability of VP-16 to directly activate caspase-8 processing (42) and of BCNU to increase Fas expression (43,44).

In addition, in accordance with previous findings demostrating the involvement of the mitochondrial-dependent pathway in Fas-induced apoptosis of Bcl-X_L-overexpressing glioma cells (45) and of ERK activation in the regulation of Bcl-X_L expression (30,46), we showed that inhibition of ERK activation by reducing Bcl-X_L levels sensitized siTRPV2-U87MG transfected cells to mitochondrial-dependent apoptosis induced by Fas triggering alone or in combination with the chemotherapeutic agents.

Our results also provide evidence that neither diminished procaspase-8 expression in TRPV2-silenced U87MG cells was reverted nor caspase-8 cleavage was induced by inhibition of ERK activation. In accordance with previous reports, these findings suggest that increased Fas levels (47,48) and reduced Bcl-X_L expression (49) do not cause detectable caspase-8 activation, although these events trigger Fas-mediated apoptosis (50).

Finally, we found that Akt/PKB was phosphorylated in U87MG cells at basal levels and that TRPV2 silencing causes a profound reduction of Akt phosphorylation status that was markedly reverted by inhibition of ERK activation. These results are consistent with previous evidence showing that PI3-kinase inhibitors inhibit calcium overload and cell death in mTRPV2-transfected cells (25). Overall, our findings indicate that ERK activation following TRPV2 silencing regulates the susceptibility of U87MG glioma cells to Fas-induced apoptosis by altering the balance between proapoptotic and antiapoptotic signals.

In conclusion, we have identified ERK activation as a key signalling event regulating proliferation and chemoresistance in glioma cells exhibiting an impaired expression of TRPV2 channel: ERK activation following TRPV2 silencing drives cell proliferation and prevents glioma cell apoptosis by repressing Fas expression and PI3K/Akt activation and promoting Bcl-X_L expression. Further investigations are required to completely understand the relationship between TRPV2 and ERK activation and Fas triggering in glioma cells.

Our findings showing that TRPV2 negatively regulates glioma cell survival and proliferation as well as resistance to Fas-induced apoptotic cell death may have important pathophysiological implications, particularly in view of loss of TRPV2 mRNA and protein expression observed during glioma progression. Understanding the role of TRPV2 in the regulation of survival and proliferation signalling pathways could shed light on the mechanisms of resistance of these cancer cells to death receptor- and chemotherapy-induced apoptosis and lead to novel approaches to primary brain tumor therapy.

Supplementary material

Supplementary Figure 1 can be found at http://carcin.oxfordjournals.org/

Funding

University of Camerino Grant 2009, AIRC Regional Grant 2007 and AIRC Regional Studentship 2009.

References

1. Kleihues,P. *et al*. (2002) The WHO classification of tumors of the nervous system. *J. Neuropathol. Exp. Neurol.*, **61**, 215–225.
2. Giese,A. *et al*. (1996) Glioma invasion in the central nervous system. *Neurosurgery*, **39**, 235–250.
3. Castro,M.G. *et al*. (2003) Current and future strategies for the treatment of malignant brain tumors. *Pharmacol. Ther.*, **98**, 71–108.
4. Ashkenazi,A. *et al*. (1998) Death receptors: signaling and modulation. *Science*, **281**, 1305–1308.
5. Scaffidi,C. *et al*. (1998) Two CD95 (APO/Fas) signaling pathways. *EMBO J.*, **16**, 1675–1687.
6. Holmström,T.H. *et al*. (2000) MAPK/ERK signalling in activated T cells inhibits CD95/Fas-mediated apoptosis downstream of DISC assembly. *EMBO J.*, **19**, 5418–5428.
7. Söderström,T.S. *et al*. (2002) Mitogen-activated protein kinase/extracellular signal-regulated kinase signaling in activated T cells abrogates TRAIL-induced apoptosis upstream of the mitochondrial amplification loop and caspase-8. *J. Immunol.*, **169**, 2851–2860.
8. Cagnol,S. *et al*. (2006) Prolonged activation of ERK 1,2 induces FADD-independent caspase 8 activation and cell death. *Apoptosis*, **11**, 337–346.
9. Fanton,C.P. *et al*. (2001) Dual growth arrest pathways in astrocytes and astrocytic tumors in response to Raf-1 activation. *J. Biol. Chem.*, **276**, 18871–18877.
10. Marshall,C.J. (1994) MAP kinase kinase kinase, MAP kinase kinase and MAP kinase. *Curr. Opin. Genet. Dev.*, **4**, 82–89.
11. Bonni,A. *et al*. (1999) Cell survival promoted by the Ras-MAPK signalling pathway by transcription-dependent and –independent mechanisms. *Science*, **286**, 1358–1362.
12. Erhardt,P. *et al*. (1999) B-Raf inhibits programmed cell death downstream of cytochrome c release from mitochondria by activating the MEK/Erk pathway. *Mol. Cell. Biol*, **19**, 5308–5315.
13. Wilson,D.J. *et al*. (1999) MEK1 activation rescues Jurkat T cells from Fas-induced apoptosis. *Cell. Immunol.*, **194**, 67–77.
14. Bödding,M. (2007) TRP proteins and cancer. *Cell Signal*, **19**, 617–624.
15. Prevarskaya,N. *et al*. (2007) TRP channels in cancer. *Biochim. Biophys. Acta*, **1772**, 937–946.
16. Amantini,C. *et al*. (2007) Capsaicin-induced apoptosis of glioma cells is mediated by TRPV1 vanilloid receptor and requires p38 MAPK activation. *J. Neurochem*, **102**, 977–990.

17. Caterina,M.J. *et al*. (1999) A capsaicin-receptor homologue with a high threshold for noxious heat. *Nature*, **398**, 436–441.
18. Muraki,K. *et al*. (2003) TRPV2 is a component of osmotically sensitive cation channels in murine aortic myocytes. *Circ. Res.*, **93**, 829–838.
19. Zimmermann,K. *et al*. (2005) The TRPV1/2/3 activator 2-aminoethoxydiphenyl borate sensitizes native nociceptive neurons to heat in wild type but not TRPV1 deficient mice. *Neuroscience*, **135**, 1277–1284.
20. Qin,N. *et al*. (2008) TRPV2 is activated by cannabidiol and mediates CGRP release in cultured rat dorsal root ganglion neurons. *J. Neurosci.*, **28**, 6231–6238.
21. Kowase,T. *et al*. (2002) Immunohistochemical localization of growth factor-regulated channel (GRC) in human tissues. *Endocr. J.*, **49**, 349–355.
22. Saunders,C.I. *et al*. (2007) Expression of transient receptor potential vanilloid 1 (TRPV1) and 2 (TRPV2) in human peripheral blood. *Mol. Immunol.*, **44**, 1429–1435.
23. Caprodossi,S. *et al*. (2008) Transient receptor potential vanilloid type 2 (TRPV2) expression in normal urothelium and in urothelial carcinoma of human bladder: correlation with the pathologic stage. *Eur. Urol.*, **54**, 612–620.
24. Kanzaki,M. *et al*. (1999) Translocation of a calcium-permeable cation channel induced by insulin-like growth factor-I. *Nat. Cell Biol*, **1**, 165–170.
25. Penna,A. *et al*. (2006) PI3-kinase promotes TRPV2 activity independently of channel translocation to the plasma membrane. *Cell Calcium*, **39**, 495–507.
26. Iwata,Y. *et al*. (2003) A novel mechanism of myocyte degeneration involving the Ca^{2+}-permeable growth factor-related channel. *J. Cell Biol.*, **161**, 957–967.
27. Monet,M. *et al*. (2009) Lysophospholipids stimulate prostate cancer cell migration via TRPV2 channel activation. *Biochim. Biophys. Acta.*, **1793**, 528–539.
28. Mandell,J.W. *et al*. (1998) In situ visualization of intratumor growth factor signaling: immunohistochemical localization of activated ERK/MAP kinase in glial neoplasms. *Am. J. Pathol.*, **153**, 1411–1423.
29. Pardo,O.E. *et al*. (2002) Fibroblast growth factor-2 induces translational regulation of Bcl-XL and Bcl-2 via a MEK-dependent pathway. *J. Biol. Chem.*, **277**, 12040–12046.
30. Lee,J.T. *et al*. (2007) Akt inactivates ERK causing decreased response to chemotherapeutic drugs in advanced CaP cells. *Cell Cycle*, **7**, 631–636.
31. Manning,B.D. *et al*. (2007) AKT/PKB signaling: navigating downstream. *Cell*, **129**, 1261–1274.
32. Yount,G.L., Levine,K.S., Kuriyama,H., Haas-Kogan,D.A. and Israel,M.A. (1999) Fas (APO-1/CD95) signalling pathway is intact in radioresistant human glioma cells. *Cancer Res.*, **59**, 1362–1365.
33. Nagane,M. *et al*. (1998) Drug resistance of human glioblastoma cells conferred by a tumor-specific mutant epidermal growth factor receptor through modulation of Bcl-XL and caspase-3-like proteases. *Proc. Natl Acad. Sci. USA*, **10**, 5274–5279.
34. Mcferrin,M.B. *et al*. (2006) A role for ion channels in glioma invasion. *Neuron Glia Biol.*, **2**, 39–49.
35. Huang,L. *et al*. (2009) ATP-sensitive potassium channels control glioma cells proliferation by regulating ERK activity. *Carcinogenesis*, **30**, 737–744.
36. Katsetos,C.D. *et al*. (2003) Class III beta-tubulin isotype: a key cytoskeletal protein at the crossroads of developmental neurobiology and tumor neuropathology. *J. Child Neurol.*, **18**, 851–866.
37. Giraud,S. *et al*. (2007) In vitro apoptotic introduction of human glioblastoma cells by Fas ligand plus etoposide and in vivo antitumour activity of combined drugs in xenografted nude rats. *Int. J. Oncol.*, **30**, 273–281.
38. Shaul,Y.D. *et al*. (2007) The MEK/ERK cascade from signaling specificity to diverse functions. *Biochim. Biophys. Acta.*, **1773**, 1213–1226.
39. Walker,L.S. *et al*. (1999) Lack of activation induced cell death in human T blast despite CD95L up-regulation: protection from apoptosis by MEK signalling. *Immunology*, **98**, 569–575.
40. Kalas,W. *et al*. (2002) Inhibition of MEK induces Fas expression and apoptosis in lymphomas overexpressing Ras. *Leuk. Lymphoma*, **43**, 1469–1474.
41. Lind,C.R. *et al*. (2006) The mitogen-activated/extracellular signal-regulated kinase kinase 1/2 inhibitor U0126 induces glial fibrillary acid protein expression and reduces the proliferation and migration of C6 glioma cells. *Neuroscience*, **141**, 1925–1933.
42. Boesen-de Cock,J.G. *et al*. (1998) The anti-cancer drug etoposide can induce caspase-8 processing and apoptosis in absence of CD95 receptor-ligand interaction. *Apoptosis*, **3**, 17–25.
43. Röhn,T.A. *et al*. (2001) CCNU-dependent potentiation of TRAIL/Apo2L-induced apoptosis in human glioma cells is p53-independent but may involve enhanced cytochrome c release. *Oncogene*, **20**, 4128–4137.
44 Roos,W. *et al*. (2004) Apoptosis triggered by DNA damage 06-methylguanine in human lymphocytes requires DNA replication and is mediated by p53 and Fas/CD95/Apo-1. *Oncogene*, **23**, 359–367.
45. Decaudin,D. *et al*. (1997) Bcl-2 and Bcl-XL antagonize the mitochondrial dysfunction preceding nuclear apoptosis induced by chemotherapeutic agents. *Cancer Res.*, **57**, 62–67.
46. Jost,M. *et al*. (2001) Epidermal growth factor receptor-dependent control of keratinocyte survival and Bcl-xL expression through a MEK-dependent pathway. *J. Biol. Chem.*, **276**, 6320–6326.
47. Feng,H. *et al*. (2004) Evidence for a novel caspase-8-independent, Fas death domain-mediated apoptotic pathway. *J. Biomed. Biotechnol.*, **2004**, 41–51.
48. Zhang,L. *et al*. (2004) A caspase-8-independent signalling pathway activated by Fas ligation leads to exposure of the Bak N terminus. *J. Biol. Chem.*, **279**, 33865–33874.
49. Luo,X. *et al*. (1998) Bid, a Bcl2 interacting protein, mediates cytochrome c release from mitochondria in response to activation of cell surface death receptors. *Cell*, **94**, 481–490.
50. Belka,C. *et al*. (2000) Differential role of caspase-8 and BID activation during radiation- and CD95-induced apoptosis. *Oncogene*, **19**, 1181–1190.

Received November 19, 2009; revised January 13, 2010; accepted January 16, 2010